Int. J. Solids Structures Vol. 29, No. 12, pp. 1567–1579, 1992
Printed in Great Britain.

0020-7683/92 $5.00 + .00

FINITE ELEMENTS FOR DYNAMIC MODELING OF UNIAXIAL RODS WITH FREQUENCY-DEPENDENT MATERIAL PROPERTIES

GEORGE A. LESIEUTRE
Department of Aerospace Engineering, The Pennsylvania State University, 233 Hammond, University Park, PA 16802, U.S.A.

(*Received* 10 *April* 1991; *in revised form* 16 *September* 1991)

Abstract—New developments in a method of modeling frequency-depedent material damping and modulus in structural dynamics analysis are reported. The fundamental feature of the general method is the introduction of augmenting thermodynamic fields (ATF) to interact with the mechanical displacement field of continuum mechanics. These ATF are directly motivated by the "internal state variables" of materials science. The coupled partial differential equations which govern the dynamic behavior of a uniaxial rod are numerically solved within the computational framework of the finite element method, resulting in "ATF-damped" finite elements. Previous work in the development of this modeling technique is characterized by the use of a single augmenting field, with application to lightly-damped rods, beams and truss structures. New developments include: (1) demonstration of the ability to model the behavior of high-damping materials; and (2) the use of multiple augmenting fields to model materials whose behavior departs significantly from that of standard anelastic solids.

NOMENCLATURE

$A(x)$	affinity, thermodynamically conjugate to augmenting thermodynamic field
$\mathbf{A}$	ATF first-order element or system matrix ("augmented mass matrix")
B	inverse of the relaxation time constant at constant strain
$\mathbf{B}$	ATF zeroth-order element or system matrix ("augmented stiffness matrix")
$\mathbf{B}$	coupling matrix that relates $\mathbf{p}$ to equations of evolution for $\mathbf{q}$
E^*	complex modulus
E'	storage modulus
E''	loss modulus
E_r	relaxed (low-frequency) Young's modulus
E_u	unrelaxed (high-frequency) Young's modulus
L	constant of proportionality between the rate of change of an augmenting field and the corresponding affinity
L_T	total length of rod
$\mathbf{p}$	vector of discrete ATF displacements
$\mathbf{q}$	vector of discrete mechanical displacements
$u(x)$	mechanical longitudinal displacement field for uniaxial rod element
x	independent variable for uniaxial rod element, reference position of mass particle
$\mathbf{x}$	vector of element or global degrees of freedom (combines $\mathbf{p}$ and $\mathbf{q}$)
α	material property that couples an augmenting field to the longitudinal normal stress
δ	material property that couples an augmenting field to the corresponding affinity
Δ	relaxation magnitude
$\varepsilon(x)$	longitudinal normal strain field in uniaxial rod element
η	frequency-dependent material loss factor, ratio of loss modulus to storage modulus
$\gamma(x)$	augmenting field, gradient of $\xi(x)$
λ	complex eigenvalue
ρ	mass density in the reference configuration
$\sigma(x)$	longitudinal normal stress field in uniaxial rod element
ω	radian frequency
$\xi_i(x)$	ith augmenting thermodynamic field (ATF)
ζ	modal damping ratio.

1. INTRODUCTION

Vibration damping is essential to the attainment of performance goals for a variety of advanced engineering systems. In common built-up structures which operate in the atmosphere, air damping and joint damping typically dominate system damping. However, material damping can also be an important contributor to overall damping in many applications, such as precision spacecraft structures in orbit. While considerable effort has

gone into the development of high-damping non-structural and structural materials for use in aerospace vibration control, sensitivity to temperature and frequency complicates their use. The development of analytical tools capable of dealing directly with frequency-dependent material properties in particular is an area of current research with potential for high pay-off.

Current popular treatments of damping in structural dynamics are unable to reproduce the fundamental frequency-dependent behavior of real materials. However, structural dynamicists are the unintended beneficiaries of a sizable literature on material damping (Ashley, 1982). For many years, crystallographers and metallurgists have used "internal friction" as a probe into the underlying structure of materials. By measuring damping as a function of frequency, temperature, deformation type and amplitude, they have investigated the mobility and activation energies of various microstructural features of materials. These researchers have identified a multitude of internal variables and relaxation mechanisms that range, in geometrical scale, from crystal lattice dimensions to structural dimensions and, in temporal scale, over a similarly broad range (Nowick and Berry, 1972; Zener, 1948).

This observation provided the motivation for the initial development of the augmenting thermodynamic fields (ATF) modeling method (Lesieutre and Mingori, 1990; Lesieutre, 1989)—a time-domain continuum model of material damping that preserves the characteristic frequency-dependent behavior of real materials (damping and modulus)—a physically-motivated model fully compatible with current finite element structural analysis methods. This paper reports new developments in the ATF modeling method, specifically the capabilities to model the behavior of high-damping materials and, through the use of multiple augmenting fields, the behavior of materials that depart significantly from that of standard anelastic solids. These results indicate that the ATF method may be an effective way to accommodate frequency-dependent material properties in engineering structural design and analysis.

2. RELATED RESEARCH

Several methods for incorporating material damping into structural models have been used, and continue to be used within the engineering community. These methods include viscous damping, frequency-dependent viscous damping, complex modulus, hysteretic damping, structural damping, viscoelasticity, hereditary integrals and model damping (Bert, 1973; Hobbs, 1971). Each has some utility, but each suffers from one flaw or another. Although some potentially accurate models exist (e.g. viscoelasticity), they are not widely used in the engineering community – perhaps because of the lack of physical motivation for, or the difficulty of use of, such models.

The need to better accommodate frequency-dependent material properties in engineering structural dyanamic analysis has motivated several new relevant developments. Important results in the recent literature include those reported in Golla and Hughes (1985), McTavish and Hughes (1987), Bagley and Torvik (1983), Torvik and Bagley (1987), Padovan (1987) and Segalman (1987).

Golla, Hughes and McTavish (GHM) developed a time-domain finite element treatment of linear viscoelasticity that is most closely related to the subject ATF method. The ATF method is primarily distinguished from the GHM approach in that it is a direct time-domain formulation, amenable to numerical treatment using conventional finite element methods. Like ATF, GHM employs additional coordinates to more accurately model damping. However, the "dissipation coordinates" of GHM are internal to individual elements, while the augmenting thermodynamic fields of ATF are continuous from element to element.

The core of Bagley and Torvik's material damping model is the use of fractional time derivatives in material constitutive equations. Their development was motivated by the observation that the frequency dependence observed in real materials is often weaker than the dependence predicted by first-order viscoelastic models. Padovan recently demonstrated efficient, stable transient solution algorithms for finite element simulation of viscoelastic

problems involving fractional operators. However, the computational requirement to store a truncated time history seems tantamount to the introduction of additional coordinates.

Segalman addressed the calculation of stiffness and damping matrices for structures made from linear viscoelastic materials. His is essentially a perturbation technique that avoids the introduction of additional coordinates. The resulting stiffness and damping matrices are, however, generally unsymmetric, and the assumption of "small viscoelasticity" is likely to limit the utility of the approach.

In recent years, the modal strain energy (MSE) modeling method for estimating the damping of materials and structures from the measured damping of constituent materials has continued to grow. However, all of the preceding approaches have advantages over this now-conventional MSE method in that they are time-domain models, modal damping may be calculated concurrently with model frequency (no look-up tables or iterative procedures are required to converge on both), and the resulting complex modes more accurately reflect the relative phase of vibration at various points on a structure.

3. UNIAXIAL ROD VIBRATION

As previously noted, the physically-significant "internal state variables" of materials science play a central role in this work, motivating the introduction of augmenting thermodynamic fields (ATF) to interact with the mechanical displacement field. Coupled material constitutive relations and partial differential equations (PDE) of evolution are developed for a uniaxial structural rod and the PDE are solved numerically using the finite element method.

The results of an investigation of two cases of interest are described herein. The first case addresses the applicability of the ATF modeling method to high-damping materials, while the second addresses the use of multiple augmenting fields to approximate material behavior that exhibits frequency-dependence weaker than that of a standard anelastic solid. In both cases, Fourier analysis yields an equation for the effective complex modulus of a material described using augmenting fields, and the resulting expected relationship between damping and frequency is verified through finite element solution of free vibration eigenvalue problems.

3.1. *High damping materials: single ATF*

3.1.1. *Governing equations.* Consider the case of one-dimensional motion, corresponding to longitudinal vibration of a thin rod. The mechanical displacement along the rod is denoted by $u(x)$, the longitudinal normal strain by $\varepsilon(x) = u'(x)$, and the rod has uniform mass density ρ and unrelaxed modulus of elasticity E_u. A single augmenting thermodynamic field, $\xi(x)$, is introduced. The fields thermodynamically conjugate to $\varepsilon(x)$ and $\xi(x)$ are the stress, $\sigma(x)$, and the affinity, $A(x)$. The affinity can be interpreted as a thermodynamic "force" driving ξ towards equilibrium. The material property δ describes the strength of the coupling of the two dependent fields, u and ξ. Analogously, α is the material property that relates local changes in A to those in ξ. Following Nowick and Berry (1972) and Lesieutre and Mingori (1990), the material constitutive equations may be found as:

$$\sigma = E_u\varepsilon - \delta\xi$$

$$A = \delta\varepsilon - \alpha\xi.$$

The usual one-dimensional stress–strain constitutive relations are seen to be augmented by an additional term in ξ. The equation of evolution for the mechanical displacement field is developed from consideration of momentum balance (with zero body forces assumed). The equation of evolution for the augmenting thermodynamic field, $\xi(x)$, is found by assuming that the local rate of change of ξ is proportional to A or, equivalently, that the rate of change of ξ is proportional to its deviation from a local equilibrium value, $\bar{\xi}$ (that value of ξ at which $A = 0$). The result is a first-order differential equation:

$$\dot{\xi} = LA = -B(\xi - \bar{\xi}) = -B\left(\xi - \left(\frac{\delta}{\chi}\right)\varepsilon\right).$$

This is a relaxation equation, and describes how the augmenting field evolves towards a new equilibrium state through a finite-rate kinetic process. The material property B is the inverse of the relaxation time constant (at constant strain). A material modeled using a single augmenting field is essentially a continuum version of a standard anelastic solid.

The resulting partial differential equations of evolution couple u and ξ:

$$\begin{aligned} \rho\ddot{u} - E_u u'' &= -\delta\xi' \\ \dot{\xi} + B\xi &= \left(\frac{B\delta}{\chi}\right)u'. \end{aligned} \tag{1}$$

A bilinear variational principle that generates these equations has also been developed (Lesieutre, 1992), and it leads to insight concerning the boundary conditions on the mechanical displacement and augmenting thermodynamic fields. The augmenting thermodynamic field is essentially an internal field, i.e. there are no explicit boundary conditions that it alone must satisfy. However, the mechanical displacement field must satisfy either displacement ("geometric") or stress ("natural") boundary conditions at each end of the rod, as is the case in undamped structural dynamics. Note that the stress boundary condition does involve the augmenting field, ξ.

As shown in Lesieutre (1989) for small damping, the damping and effective modulus for a material described by eqns 1 are frequency-dependent. An approximate equation for the loss factor, η, is:

$$\eta = \frac{1}{2}\left(\frac{\delta^2}{E_u \chi}\right)\frac{2\left(\frac{\omega}{B}\right)}{\left(1 + \left(\frac{\omega}{B}\right)^2\right)}.$$

The peak loss factor is approximately equal to $\delta^2/2E_u\chi$ and is observed at $\omega = B$.

For an arbitrary level of damping, similar analysis results in the following expression for the complex modulus of the material:

$$E^* = E' + iE'' = \left(E_u - \frac{\delta^2/\chi}{1 + (\omega/B)^2}\right) + i\left((\delta^2/\chi)\frac{(\omega/B)}{1 + (\omega/B)^2}\right).$$

Defining the relaxed (low-frequency) modulus, E_r, as:

$$E_r = E_u - \frac{\delta^2}{\chi}$$

and the relaxation strength, Δ, as:

$$\Delta = \frac{\delta^2}{E_r \chi},$$

the expression for the complex modulus may be expressed alternatively as:

$$E^* = E_r\left(1+\Delta\frac{(\omega/B)^2}{1+(\omega/B)^2}\right)+iE_r\left(\Delta\frac{(\omega/B)}{1+(\omega/B)^2}\right).$$

The loss factor may subsequently be found as the ratio of the loss modulus to the storage modulus:

$$\eta = \frac{\Delta(\omega/B)}{1+(1+\Delta)(\omega/B)^2} = \eta_{\max}\left(\frac{2(\omega/\bar{B})}{1+(\omega/\bar{B})^2}\right) \tag{2a}$$

where the peak loss factor, $\eta_{\max}$, and frequency at which this peak is observed, $\bar{B}$, are given by:

$$\eta_{\max} = \frac{\Delta}{2(1+\Delta)^{1/2}} \quad \text{and} \quad \bar{B} = \frac{B}{(1+\Delta)^{1/2}}. \tag{2b}$$

These results are identical to those presented in (Nowick and Berry, 1972) for a standard anelastic solid. Light coupling between the mechanical displacement field and the augmenting thermodynamic field results in small damping, with a peak loss factor of approximately half the relaxation strength, at a frequency equal to the inverse of the relaxation time at constant strain. As is seen from the preceding result for larger coupling, the peak loss factor is less than half the relaxation strength and is observed at a lower frequency.

Note that no special physical interpretation or units need be given to the augmenting field in order to use this modeling method given experimental data. In that case, the relaxation strength and time may be determined from the data, the material property B from the second of eqn 2b, and properties α and δ from the first of eqns 2b (non-uniquely).

As described in Lesieutre and Mingori (1990), an alternate form of the governing equations for uniaxial vibration may be developed and used to advantage in the formulation of finite elements. In terms of γ, the gradient of the ξ-field, the equations may be expressed as follows:

$$\begin{aligned} \rho\ddot{u} - Eu'' &= -\delta\gamma \\ \dot{\gamma} + B\gamma &= \left(\frac{B\delta}{\alpha}\right)u''. \end{aligned} \tag{3}$$

This formulation contains only even spatial derivatives, a result which leads to some benefits in numerical solution, such as symmetric element submatrices and good approximation of the relative magnitudes of the imaginary and real parts of complex eigenvalues (even when the absolute magnitude is not well-approximated).

3.1.2. *Finite element treatment.* Previous work (Lesieutre, 1989) has shown the u-γ form of the governing equations (eqn 3) to be superior to the u-ξ form (eqn 1), in terms of convergence of finite element solutions, and is employed exclusively herein. The reason for the better performance is not fully understood as of this writing, but may have to do with consistent interpolation of the displacement and augmenting fields.

Consider a single element of length L and cross-sectional area A, as shown in Fig. 1. The mechanical displacement field over the element $u(x)$, is approximated using a linearly-varying interpolation function, and the augmenting field, $\gamma(x)$, is similarly approximated. As described in detail in Lesieutre, (1989), the method of weighted residuals (MWR) is used to develop element matrices. The same functions used to approximate the behavior of the dependent fields in the spatial region bounded by the element are used as weighting functions. Because it can reduce the order and continuity required of assumed approximate displacement fields, integration by parts is an important part of the process of developing

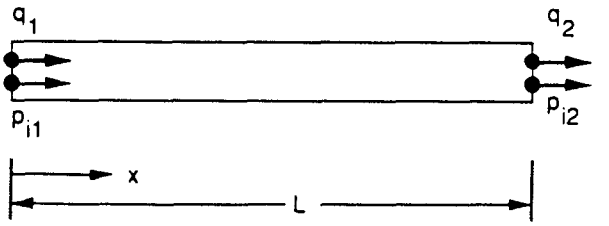

Mechanical displacement field

$$u(x)=\left[\left(1-\frac{x}{L}\right)\quad\left(\frac{x}{L}\right)\right]\begin{Bmatrix}q_1\\q_2\end{Bmatrix}$$

Augmenting thermodynamic fields

$$\gamma_i(x)=\left[\left(1-\frac{x}{L}\right)\quad\left(\frac{x}{L}\right)\right]\begin{Bmatrix}p_{i1}\\p_{i2}\end{Bmatrix}$$

Fig. 1. The linear–linear u–γ finite element.

element matrices in MWR, and is used here. Integrating the weighted equations over the length of the element and minimizing the residual leads to the following elemental matrix equations of evolution:

$$\mathbf{M}\ddot{\mathbf{q}}+\mathbf{K}\mathbf{q}=-\mathbf{B}\mathbf{p}$$

$$\mathbf{C}\dot{\mathbf{p}}+\mathbf{H}\mathbf{p}=-\mathbf{F}\mathbf{q}$$

where $\mathbf{q}$ is the vector of nodal mechanical displacements and $\mathbf{p}$ is the vector of nodal ATF displacements.

If the elemental degrees of freedom are ordered to facilitate assembly as:

$$\mathbf{x}=[\dot{q}_1\quad q_1\quad p_1\,|\,\dot{q}_2\quad q_2\quad p_2]^T$$

the elemental equations may be expressed alternatively in first-order form as:

$$\mathbf{A}\dot{\mathbf{x}}+\mathbf{B}\mathbf{x}=\mathbf{0}$$

where the element matrices for AFT-damped uniaxial rod finite elements are:

$$\mathbf{A}=\begin{bmatrix}\left(\frac{\rho AL}{3}\right) & 0 & 0 & \left(\frac{\rho AL}{6}\right) & 0 & 0\\ 0 & 1 & 0 & 0 & 0 & 0\\ 0 & 0 & \left(\frac{AL}{3}\right) & 0 & 0 & \left(\frac{AL}{6}\right)\\ \left(\frac{\rho AL}{6}\right) & 0 & 0 & \left(\frac{\rho AL}{3}\right) & 0 & 0\\ 0 & 0 & 0 & 0 & 1 & 0\\ 0 & 0 & \left(\frac{AL}{6}\right) & 0 & 0 & \left(\frac{AL}{3}\right)\end{bmatrix},$$

$$\mathbf{B} = \begin{bmatrix} 0 & \left(\frac{E_u A}{L}\right) & \left(\frac{\delta AL}{3}\right) & 0 & \left(-\frac{E_u A}{L}\right) & \left(\frac{\delta AL}{6}\right) \\ -1 & 0 & 0 & 0 & 0 & 0 \\ 0 & \left(\frac{B\delta A}{\alpha L}\right) & \left(\frac{BAL}{3}\right) & 0 & \left(-\frac{B\delta A}{\alpha L}\right) & \left(\frac{BAL}{6}\right) \\ 0 & \left(-\frac{E_u A}{L}\right) & \left(\frac{\delta AL}{6}\right) & 0 & \left(\frac{E_u A}{L}\right) & \left(\frac{\delta AL}{3}\right) \\ 0 & 0 & 0 & -1 & 0 & 0 \\ 0 & \left(-\frac{B\delta A}{\alpha L}\right) & \left(\frac{BAL}{6}\right) & 0 & \left(\frac{B\delta A}{\alpha L}\right) & \left(\frac{BAL}{3}\right) \end{bmatrix}. \tag{4}$$

In order to evaluate the performance of this formulation of the ATF-damped rod element with high damping, a specific boundary-value eigenvalue problem is addressed, namely, the determination of the natural modes of longitudinal vibration of a free-free rod. The results are compared to those expected on the basis of the approximate analysis described in the preceding section. Element matrices are assembled into global system matrices (**A** and **B**) using the usual "direct stiffness" technique of structural finite element analysis.

Assuming a solution for $\mathbf{x}(t)$ in the form $e^{\lambda t}$, the following eigenvalue problem is defined:

$$[\lambda \mathbf{A} + \mathbf{B}]\mathbf{x} = \mathbf{0}.$$

The matrix equations of motion are formulated and this problem solved to yield complex eigenvalues, λ, and eigenvectors, $\mathbf{x}$. The damping ratio for each mode is calculated as the ratio of the negative of the real part of the eigenvalue to the total magnitude. The modal damping ratio, ζ, is then plotted against the imaginary part of the eigenvalue. As noted in Lesieutre (1989), the spectrum of eigenvalues generally contains "vibration modes", "relaxation modes" and "rigid-body modes". In the complex plane, the damped vibration modes lay near the imaginary axis, slightly in the left half plane with negative real parts; the relaxation modes lie on the negative real axis. These relaxation modes are characteristic of the response of the γ field.

Two specific cases were considered numerically: (1) "light" coupling, with a relaxation strength of 0.125; and (2) "strong" coupling, with a relaxation strength of 1.25. The numerical parameter values used for this example problem were (in arbitrary, consistent units):

A = 1.0
E_u = 10.0 (in "light coupling" case)
20.0 (in "strong coupling" case, gives the same E_r)
ρ = 1.
B = 10.0
$\alpha = \delta$ = 10/9 ("light coupling")
100/9 ("strong coupling")
L_r = 1.0 (nominal total length of rod; other lengths ranging from 0.1 to 10.0 were also used to shift the modal frequencies up or down, respectively).

Figure 2 shows typical numerical results yielded by this approach, using 10 damped rod elements. Each point indicates the frequency and damping of a single vibration mode. In order to determine the modal damping ratios over a wide range of frequencies, several rod lengths were used, shifting the modal frequencies. This shifting is apparent in Fig. 2 as two groups of modes for each case, one below the frequency at which peak damping is observed, and one above.

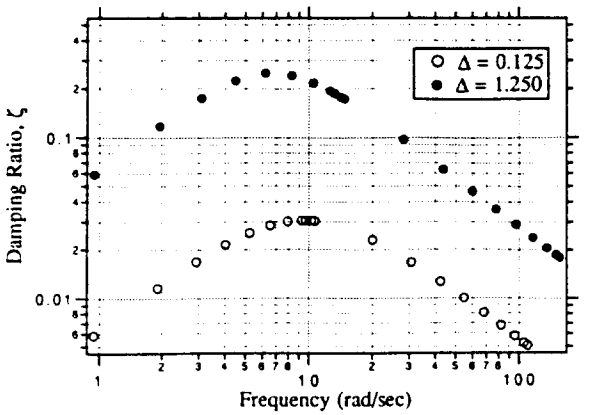

Fig. 2. Comparison of frequency-dependence of modal damping ratios for weak and strong coupling with a single augmenting field—materials have the same unrelaxed moduli and relaxation time.

The numerical finite element results of the boundary-value eigenvalue problem agree quite well with those expected on the basis of the material properties. For the light coupling case, the peak damping ratio compares well with the predicted value of 0.031, and is observed at the predicted value of 10. For stronger coupling, the peak damping ratio agrees well with the predicted value of 0.26, and is observed at the predicted value of 6.7. Note that while the relaxed (low-frequency) modulus is identical in both cases, the unrelaxed (high-frequency) modulus is a factor of 2 higher for the case of strong coupling. The effect, apparent in the finite element results, is that the ratio of modal frequencies for the case with stronger coupling to the case with light coupling is equal to 1 at low frequencies, and approaches $\sqrt{2}$ at high frequencies. The ATF modeling technique evidently captures the essential frequency-dependence of material modulus as well as that of damping.

The modal frequencies calculated from the finite element analysis only approximate the actual solutions to the PDE, with accuracy generally decreasing with increasing mode number and increasing with the number of elements. As noted previously, the use of the u–γ form of the governing equations with linear-interpolation in finite element analysis apparently preserves the relative magnitudes of the imaginary and real parts of complex eigenvalues, even when the absolute magnitude is not well-approximated. The u–ξ form of the equations, similarly interpolated, does not, even though the solutions converge to the same eigenvalues as the number of elements is increased.

The relationship between loss factor and modal damping ratio with strong coupling is, in general, complicated and depends on the specific constitutive law used to describe material behavior. For a standard anelastic solid, the peak modal damping ratio may be found using the following procedure [adapted from Nowick and Berry (1972)]:

(1) Determine the peak loss factor using the first of eqns 2b.
(2) Determine the corresponding peak loss angle using:

$$\phi_{max} = \tan^{-1}(\eta_{max}) \quad \text{(exact)}.$$

(3) Estimate the peak log decrement, δ_{max}, using the following equation with a first-order correction term:

$$\delta_{max} = \pi(1 - \sqrt{1 - 2\phi_{max}}) \quad \text{(approximate)}.$$

(4) Determine the peak modal damping ratio using:

$$\zeta_{max} = \left(\frac{\delta_{max}^2}{\delta_{max}^2 + (2\pi)^2}\right)^{1/2} \quad \text{(exact)}.$$

3.2. *Multiple augmenting fields*

3.2.1. *Governing equations.* In this section, the use of multiple ATF is considered, the motivation being to better approximate experimental data for engineering materials. As previously noted, these materials often exhibit properties with frequency-dependence weaker than that of standard anelastic solids. The development follows that of the preceding section, but introduces N augmenting fields to interact with the mechanical displacement field. The material constitutive relations take the form:

$$\sigma = E_u \varepsilon - \sum_{i=1}^{N} \delta_i \xi_i$$

$$A_i = \delta_i \varepsilon - \alpha_i \xi_i$$

where the ξ_i are "normal internal variables" (Nowick and Berry, 1972) and are not coupled to one another.

The relaxation equations for each ξ_i take the form:

$$\dot{\xi}_i = -B_i\left(\xi_i - \left(\frac{\delta_i}{\alpha_i}\right)\varepsilon\right).$$

The governing partial differential equations in terms of the γ_i and the gradients of the ξ_i, are:

$$\rho\ddot{u} - Eu'' = -\sum_{i=1}^{N} \delta_i \gamma_i$$

$$\dot{\gamma}_i + B_i \gamma_i = \left(\frac{B_i \delta_i}{\alpha_i}\right) u''. \tag{5}$$

Note that the relationship between E_r and E_u may now be expressed as:

$$E_u = E_r\left(1 + \sum_{i=1}^{N} \Delta_i\right)$$

where the individual ATF relaxation strengths, Δ_i, are given by:

$$\Delta_i = \frac{\delta_i^2}{E_r \alpha_i}.$$

In addition, the complex modulus may be expressed as:

$$E^* = E_r\left(1 + \sum_{i=1}^{N} \Delta_i \frac{(\omega/B_i)^2}{1 + (\omega/B_i)^2}\right) + iE_r\left(\sum_{i=1}^{N} \Delta_i \frac{(\omega/B_i)}{1 + (\omega/B_i)^2}\right).$$

3.2.2. *Finite element treatment.* The preceding form of the governing equations (eqn 5) is used as the starting point for the development of finite element matrices. An extension of the technique described in the earlier section for a single ATF is used, introducing additional approximating and weighting functions as appropriate. If the elemental degrees of freedom are ordered as:

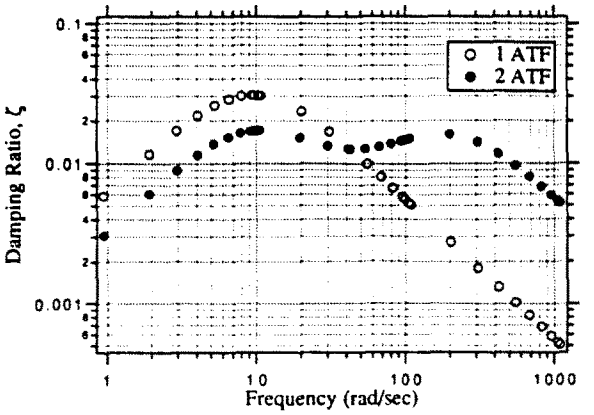

Fig. 3. Comparison of frequency-dependence of modal damping ratios using one and two augmenting fields—materials have the same asymptotic moduli.

$$\mathbf{x} = [\dot{q}_1 \quad q_1 \,|\, p_{1_1} \quad p_{2_1} \cdots p_{N_1} \,|\, \dot{q}_2 \quad q_2 \,|\, p_{1_2} \quad p_{2_2} \cdots p_{N_2}]^T$$

the element matrices for multiple-ATF-damped uniaxial rod finite elements can be developed and are given in the appendix.

Several numerical experiments were performed to investigate the performance of this formulation of an ATF-damped uniaxial rod element with multiple augmenting fields. Three cases were of particular interest: (1) the use of two ATF with widely separated relaxation times; (2) the achievement of a nearly constant loss factor over a broad frequency range as a means of approximating "structural" or "hysteric" damping in a time-domain dynamic model; and (3) the achievement of the typically weaker frequency-dependent loss factor characteristic of the "fractional derivative" model. Ten elements were used in all cases, while the total rod length was allowed to vary in order to change the modal frequencies as needed to investigate behavior in different regions of frequency.

Figure 3 illustrate the results obtained with the use of two augmenting fields with widely separated relaxation times, in terms of modal damping ratio versus frequency. For comparison, the results obtained using a single augmenting field are included. The material parameters were chosen to yield the same total relaxation magnitude and the same asymptotic dynamic moduli.

The numerical parameter values used for this example problem were (in arbitrary, consistent units):

$A = 1.0$
$E_0 = 10.0$
$\rho = 1.$
$B_1 = 10.0, \quad B_2 = 200$
$\Delta = 0.125$ ($\delta = \alpha = 10/9$ for one ATF)
($\delta = \alpha = 5/9$ for two ATF)
$L_T = 1.0$ (nominal total length of rod; other lengths ranging from 0.1 to 10.0 were also used to shift the modal frequencies up or down, respectively).

The contributions of the individual ATF to modal damping ratios in different frequency regions are apparent. Note also that the modal frequencies are identical in the high and low frequency ranges (consistent with identical asymptotic moduli), but differ slightly in between due to the different frequency-dependence of material moduli.

Figure 4 illustrates the results obtained with the use of three augmenting fields equally-spaced in log frequency, in terms of modal damping ratio versus frequency. The material parameters used are similar to those used in the preceding example, with the individual relaxation magnitudes equal to one another and each B_{i+1} a factor of 8.4 larger than B_i (with $B_1 = 10$). Note that the modal damping ratios are essentially flat over a significant

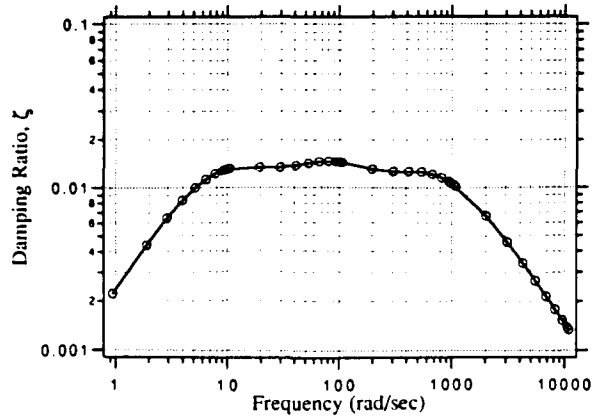

Fig. 4. Comparison of frequency-dependence of modal damping ratios using three augmenting fields—approximates "hysteretic" or "structural" damping.

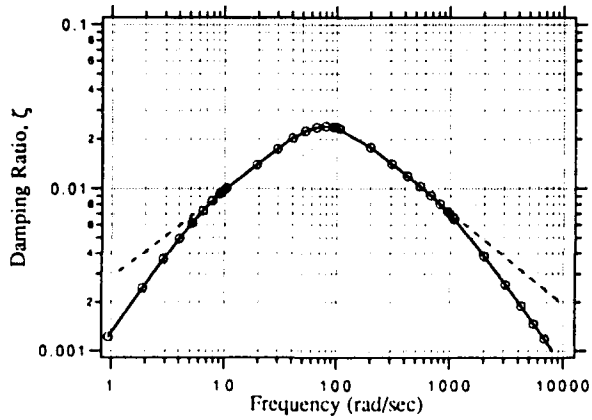

Fig. 5. Comparison of frequency-dependence of modal damping ratios using three augmenting fields—approximates "fractional derivative" behavior over a limited frequency range.

frequency range. Thus, the ATF modeling method is seen as a potential way to approximate "structural" or "hysteretic" damping in the time domain.

Figure 5 illustrates the results obtained with the use of three augmenting fields equally spaced in log frequency (by a factor of 7), in terms of modal damping ratio versus frequency. The material parameters used are similar to those used in the preceding example, with the individual relaxation magnitudes adjusted to yield apparent frequency dependence weaker than that of a comparable anelastic solid (a single ATF). The slope of the tangent dashed curve in Fig. 5 is approximately ± 0.53, considerably less than than the slope of ± 1 characteristic of the response using a single ATF. Evidently, the ATF modeling method provides a possible means of approximating the behavior of materials described by the "fractional derivative" model—albeit over a limited frequency range, but in a way that is compatible with existing finite element analysis tools.

4. SUMMARY AND CONCLUSIONS

A physically-motivated time-domain model that preserves the characteristic frequency-dependent properties of real materials, a model compatible with current computational structural analysis methods, continues to be developed. Termed the Augmenting Thermodynamic Fields (ATF) method, its key feature is the introduction of additional fields to interact with the displacement field of continuum structural dynamics.

Earlier results involving light damping achieved with a single augmenting field have been extended to high damping and the use of multiple fields. The numerical finite element results of boundary-value eigenvalue problems for longitudinal vibrations of a rod made from a single material agree quite well with those expected on the basis of the material properties. The significance of this agreement it that is may be expected to carry over into applications involving complex, irregular structures made from many materials. The results indicate that the ATF method may be an effective way to accommodate frequency-dependent material properties in engineering design and analysis.

REFERENCES

Ashley, H. (1982). On passive damping mechanisms in large space structures. *AIAA* 82-0639.

Bagley, R. L. and Torvik, P. J. (1983). Fractional calculus—a different approach to the analysis of viscoelastically damped structures. *AIAA Jl* **21**, 741–748.

Bert, C. W. (1973). Material damping: an introductory review of mathematical models, measures, and experimental techniques. *J. Sound Vibr.* **29**, 129–153.

Golla, D. F. and Hughes, P. C. (1985). Dynamics of viscoelastic structures—a time-domain, finite element formulation. *J. Appl. Mech.* **52**, 897–906.

Hobbs, G. K. (1971). Methods of treating damping in structures. *Proceedings of the 12th AIAA Structures, Structural Dynamics, and Materials Conference*, Anaheim, CA.

Lesieutre, G. A. (1989). Finite element modeling of frequency-dependent material damping using augmenting thermodynamic fields. Ph.D. dissertation, Aerospace Engineering, University of California, Los Angeles.

Lesieutre, G. A. (1992). A bilinear variational principle governing longitudinal vibration of rods with frequency-dependent material damping. *J. Appl. Mech.* (in press).

Lesieutre, G. A. and Mingori, D. L. (1990). Finite element modeling of frequency-dependent material damping using augmenting thermodynamic fields. *J. Guidance, Control, Dynamics* **13**, 1040–1050.

McTavish, D. J. and Hughes, P. C. (1987). Finite element modeling of linear viscoelastic structures. *Proceedings of the 11th ASME Biennial Conference on Mechanical Vibration and Noise*, September, 1987, Boston, MA.

Nowick, A. S. and Berry, B. S. (1972). *Anelastic Relaxation in Crystalline Solids*. Academic Press, New York.

Padovan, J. (1987). Computational algorithms for FE formulations involving fractional operators. *Comput. Mech.* **2**, 271–287.

Segalman, D. J. (1987). Calculation of damping matrices for linearly viscoelastic structures. *Proceedings of the 11th ASME Biennial Conference on Mechanical Vibration and Noise*, September, 1987, Boston, MA.

Torvik, P. J. and Bagley, R. L. (1987). Fractional derivatives in the description of damping materials and phenomena. *Proceedings of the 11th ASME Biennial Conference on Mechanical Vibration and Noise*, September, 1987, Boston, MA.

Zener, C. M. (1948). *Elasticity and Anelasticity of Metals*. University of Chicago Press, Chicago.

APPENDIX: ELEMENTAL MATRICES FOR UNIAXIAL ROD FINITE ELEMENTS WITH MULTIPLE-ATF

$$
A = \left[\begin{array}{cc:cccc:cc:cccc}
\left(\frac{\rho AL}{3}\right) & 0 & 0 & 0 & 0 & 0 & \left(\frac{\rho AL}{6}\right) & 0 & 0 & 0 & 0 & 0 \\
0 & 1 & 0 & 0 & 0 & 0 & 0 & 0 & 0 & 0 & 0 & 0 \\
\hdashline
0 & 0 & \left(\frac{AL}{3}\right)_1 & 0 & 0 & 0 & 0 & 0 & \left(\frac{AL}{6}\right)_1 & 0 & 0 & 0 \\
0 & 0 & 0 & \left(\frac{AL}{3}\right)_2 & 0 & 0 & 0 & 0 & 0 & \left(\frac{AL}{6}\right)_2 & 0 & 0 \\
0 & 0 & 0 & 0 & \ddots & 0 & 0 & 0 & 0 & 0 & \ddots & 0 \\
0 & 0 & 0 & 0 & 0 & \left(\frac{AL}{3}\right)_N & 0 & 0 & 0 & 0 & 0 & \left(\frac{AL}{6}\right)_N \\
\hdashline
\left(\frac{\rho AL}{6}\right) & 0 & 0 & 0 & 0 & 0 & \left(\frac{\rho AL}{3}\right) & 0 & 0 & 0 & 0 & 0 \\
0 & 0 & 0 & 0 & 0 & 0 & 0 & 1 & 0 & 0 & 0 & 0 \\
\hdashline
0 & 0 & \left(\frac{AL}{6}\right)_1 & 0 & 0 & 0 & 0 & 0 & \left(\frac{AL}{3}\right)_1 & 0 & 0 & 0 \\
0 & 0 & 0 & \left(\frac{AL}{6}\right)_2 & 0 & 0 & 0 & 0 & 0 & \left(\frac{AL}{3}\right)_2 & 0 & 0 \\
0 & 0 & 0 & 0 & \ddots & 0 & 0 & 0 & 0 & 0 & \ddots & 0 \\
0 & 0 & 0 & 0 & 0 & \left(\frac{AL}{6}\right)_N & 0 & 0 & 0 & 0 & 0 & \left(\frac{AL}{3}\right)_N
\end{array}\right].
$$

$$\mathbf{B} =$$

$$\left[\begin{array}{cc:ccccc:cc:ccccc}
0 & \left(\frac{E_0 A}{L}\right) & \left(\frac{\delta AL}{3}\right)_1 & \left(\frac{\delta AL}{3}\right)_2 & \cdots & \left(\frac{\delta AL}{3}\right)_N & 0 & \left(-\frac{E_0 A}{L}\right) & \left(\frac{\delta AL}{6}\right)_1 & \left(\frac{\delta AL}{6}\right)_2 & \cdots & \left(\frac{\delta AL}{6}\right)_N \\
-1 & 0 & 0 & 0 & 0 & 0 & 0 & 0 & 0 & 0 & 0 & 0 \\
\hdashline
0 & \left(\frac{B\delta A}{\chi L}\right)_1 & \left(\frac{BAL}{3}\right)_1 & 0 & 0 & 0 & 0 & \left(-\frac{B\delta A}{\chi L}\right)_1 & \left(\frac{BAL}{6}\right)_1 & 0 & 0 & 0 \\
0 & \left(\frac{B\delta A}{\chi L}\right)_2 & 0 & \left(\frac{BAL}{3}\right)_2 & 0 & 0 & 0 & \left(-\frac{B\delta A}{\chi L}\right)_2 & 0 & \left(\frac{BAL}{6}\right)_2 & 0 & 0 \\
0 & \vdots & 0 & 0 & \ddots & 0 & 0 & \vdots & 0 & 0 & \ddots & 0 \\
0 & \left(\frac{B\delta A}{\chi L}\right)_N & 0 & 0 & 0 & \left(\frac{BAL}{3}\right)_N & 0 & \left(-\frac{B\delta A}{\chi L}\right)_N & 0 & 0 & 0 & \left(\frac{BAL}{6}\right)_N \\
\hdashline
0 & \left(-\frac{E_0 A}{L}\right) & \left(\frac{\delta AL}{6}\right)_1 & \left(\frac{\delta AL}{6}\right)_2 & \cdots & \left(\frac{\delta AL}{6}\right)_N & 0 & \left(\frac{E_0 A}{L}\right) & \left(\frac{\delta AL}{3}\right)_1 & \left(\frac{\delta AL}{3}\right)_2 & \cdots & \left(\frac{\delta AL}{3}\right)_N \\
0 & 0 & 0 & 0 & 0 & 0 & -1 & 0 & 0 & 0 & 0 & 0 \\
\hdashline
0 & \left(-\frac{B\delta A}{\chi L}\right)_1 & \left(\frac{BAL}{6}\right)_1 & 0 & 0 & 0 & 0 & \left(\frac{B\delta A}{\chi L}\right)_1 & \left(\frac{BAL}{3}\right)_1 & 0 & 0 & 0 \\
0 & \left(-\frac{B\delta A}{\chi L}\right)_2 & 0 & \left(\frac{BAL}{6}\right)_2 & 0 & 0 & 0 & \left(\frac{B\delta A}{\chi L}\right)_2 & 0 & \left(\frac{BAL}{3}\right)_2 & 0 & 0 \\
0 & \vdots & 0 & 0 & \ddots & 0 & 0 & \vdots & 0 & 0 & \ddots & 0 \\
0 & \left(-\frac{B\delta A}{\chi L}\right)_N & 0 & 0 & 0 & \left(\frac{BAL}{6}\right)_N & 0 & \left(\frac{B\delta A}{\chi L}\right)_N & 0 & 0 & 0 & \left(\frac{BAL}{3}\right)_N
\end{array}\right]$$